

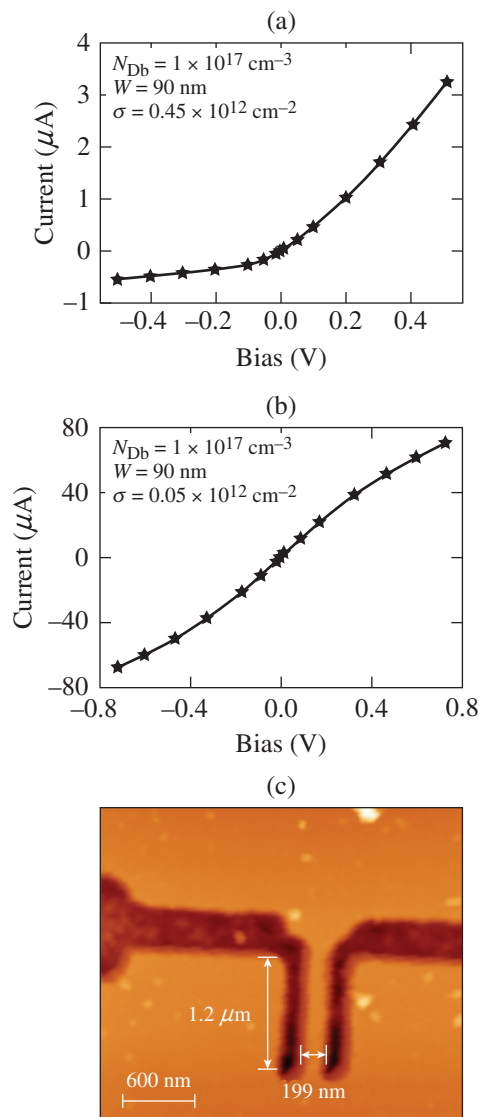
# Ultra-high Responsivity of Optically Active, Semiconducting Asymmetric Nanochannel Diodes

## Introduction

Room-temperature nanodevices based on quantum confinement and/or ballistic nonlinearities are intrinsic nanostructures, not simply scaled-down conventional circuitry, and are gaining wide-spread research attention. Among the nanodevices, one of the most popular is the asymmetric nanochannel diode (ANCD), also referred to as a self-switching diode (SSD), first proposed by Song *et al.*<sup>1</sup> ANCD's, contrary to conventional diodes, do not rely on energy-barrier concepts to achieve rectification, but rather their nonlinear current–voltage ( $I$ – $V$ ) characteristics result from the carrier transport in an asymmetric nanochannel. The ANCD planar geometry allows for a flexible design and easy integration as a multi-element sensor or with either optical nanoconcentrators or THz coupling antennas. Based on Monte Carlo (MC) simulations, ANCD's are expected to be efficient THz generators,<sup>2</sup> which have been demonstrated to be viable THz detectors.<sup>3</sup>

Typically, carrier transport in ANCD's is confined to a two-dimensional electron gas (2DEG) layer in order to take advantage of the 2DEG ultrahigh mobility and, in this way, minimize the carrier transient time. Depending on the device's dimensions and/or fabrication process and the level of its control, there are two basic types of SSD's: “normally OFF” devices with a channel open/depleted at zero bias and “normally ON” devices, where the channel is always conducting. These two types exhibit quite different  $I$ – $V$  curves, as shown in Figs. 143.42(a) and 143.42(b), where MC simulations<sup>4</sup> of two ANCD's of the same geometry are presented but with different values for the surface charge  $\sigma$ .

Despite the popularity of SSD's, extensive fundamental and applied research is still needed to fully understand their direct current (dc) and radio-frequency (rf) carrier transport through the asymmetric nanochannel, as well as their performance in both the THz and optical radiation ranges. Our work presented here focuses on photoresponse properties of ANCD's, and we demonstrate that especially normally ON devices possess a very strong, intrinsic internal photoelectron gain mechanism, making them very attractive as possible room-temperature ultrafast optical detectors with single-photon sensitivity.



E24323JR

Figure 143.42 Monte Carlo (MC) results for  $I$ – $V$  curves of an asymmetric nanochannel diode (ANCD) with a channel width  $W = 90 \text{ nm}$  and two different values of the surface charge  $\sigma$ , leading to (a) a depleted channel and diode-like characteristics, (b) a conducting channel (effective width of 80 nm at zero dc bias) and nonlinear characteristics, and (c) an atomic force microscope image of an actual device.

## Device Fabrication and Experimentation

Our tested devices consisted of  $\sim 1.2\text{-}\mu\text{m}$ -long and  $\sim 200\text{-}$  to  $300\text{-nm}$ -wide channels [see Fig. 143.42(c)] and were fabricated on an InGaAs/InAlAs quantum-well heterostructure grown on an InP wafer. The fabrication started with the formation of mesa structures by wet chemical etching with an  $\text{H}_3\text{PO}_4/\text{H}_2\text{O}_2/\text{H}_2\text{O}$ -based solution. Ohmic contacts were then formed by thermal evaporation of  $50\text{-nm}$  of Au/Ge/Ni alloy, followed by a  $200\text{-nm}$  Au layer. Finally a nanochannel was defined using electron-beam lithography and wet chemical etching.

The ANCD I–V curves were collected by measuring the transport current for the voltage-source biasing condition, both in the dark and under light illumination. For optical excitation, we used  $800\text{-nm}$ -wavelength continuous-wave (cw) radiation generated by a commercial, non-mode-locked Ti:sapphire laser. The same laser system, but in the pulsed mode, was used for time-domain response characterization studies. For these measurements, our diodes were dc biased and illuminated with a train of  $100\text{-fs}$ -wide pulses with an average power of about  $400\text{ }\mu\text{W}$ . The electrical output was registered using a bias-tee and a fast  $6\text{-GHz}$ -bandwidth sampling oscilloscope.

## Experimental Results and Analysis

Figure 143.43 presents a family of direct current I–V characteristics of a normally OFF device, measured in the dark (black dots) and with a single- $\mu\text{W}$  level of light illumination (see figure caption) focused on the device. We note that the curve measured in the dark well resembles the one presented in Fig. 143.42(a). The unbiased ANCD is clearly in the OFF state and, when biased, a diode-like characteristic is well reproduced. A leakage current at negative bias is ascribed to the relatively large channel width of this ANCD sample, while the change of the slope near  $3\text{-V}$  bias is caused, according to MC simulations, by velocity saturation associated with electron scattering from  $\Gamma$  into the  $L$  satellite valley.

The impact of the light illumination is very strong, as illustrated in the top left inset in Fig. 143.43, where we plot a family of photocurrent characteristics versus the bias voltage. The observed behavior very strongly points to optical gating of the nanochannel. In fact, the first quadrant (positive voltage and positive photocurrent) of the inset graph closely resembles the characteristics of a field-effect transistor (FET), except that here the various curves of the graph correspond to different optical intensities with a threshold optical power of about  $0.9\text{ }\mu\text{W}$ .

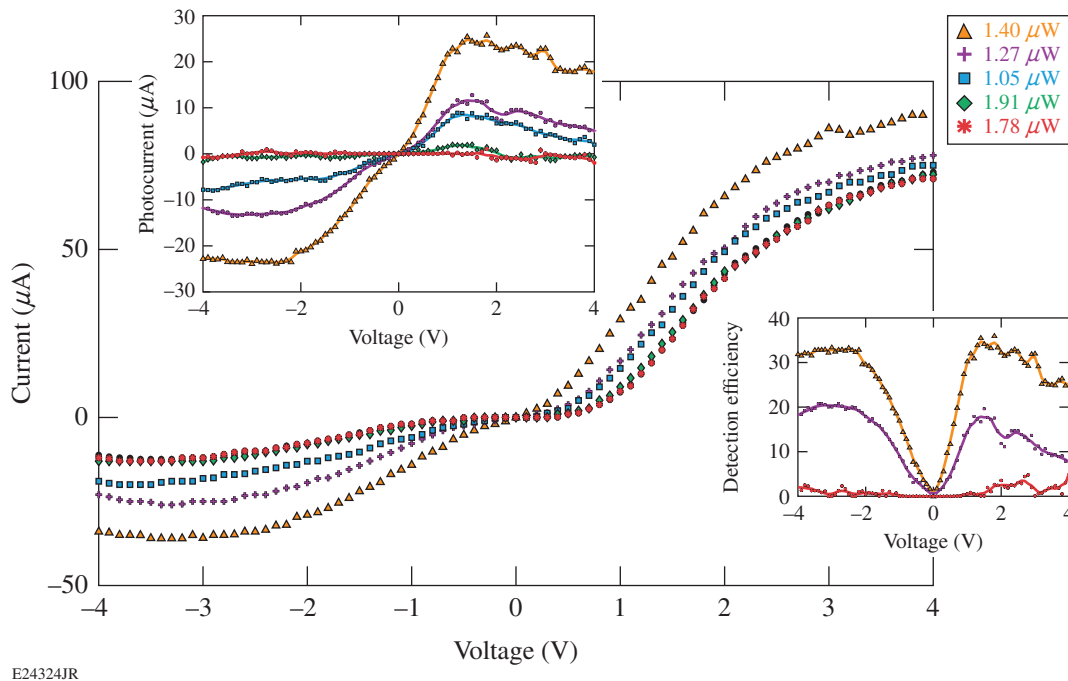


Figure 143.43

Direct-current I–V characteristics for a normally OFF device (channel width of  $\sim 200\text{ nm}$ ) in darkness (black dots) and under  $800\text{-nm}$ -wavelength cw laser illumination. The top left inset shows the photocurrent's dependence on the bias voltage, collected as the current difference between the I–V curve under a given illumination and the one measured in the dark. The bottom right inset presents the detection efficiency's (DE's) dependence on the bias voltage, calculated for a given curve as the ratio of the photocurrent to incident laser power and expressed in units of electron/photon. The legend for all presented traces is as follows: orange triangles  $1.4\text{ }\mu\text{W}$ ; purple crosses  $1.27\text{ }\mu\text{W}$ ; blue squares  $1.05\text{ }\mu\text{W}$ ; green diamonds  $0.91\text{ }\mu\text{W}$ ; and red stars  $0.78\text{ }\mu\text{W}$ .

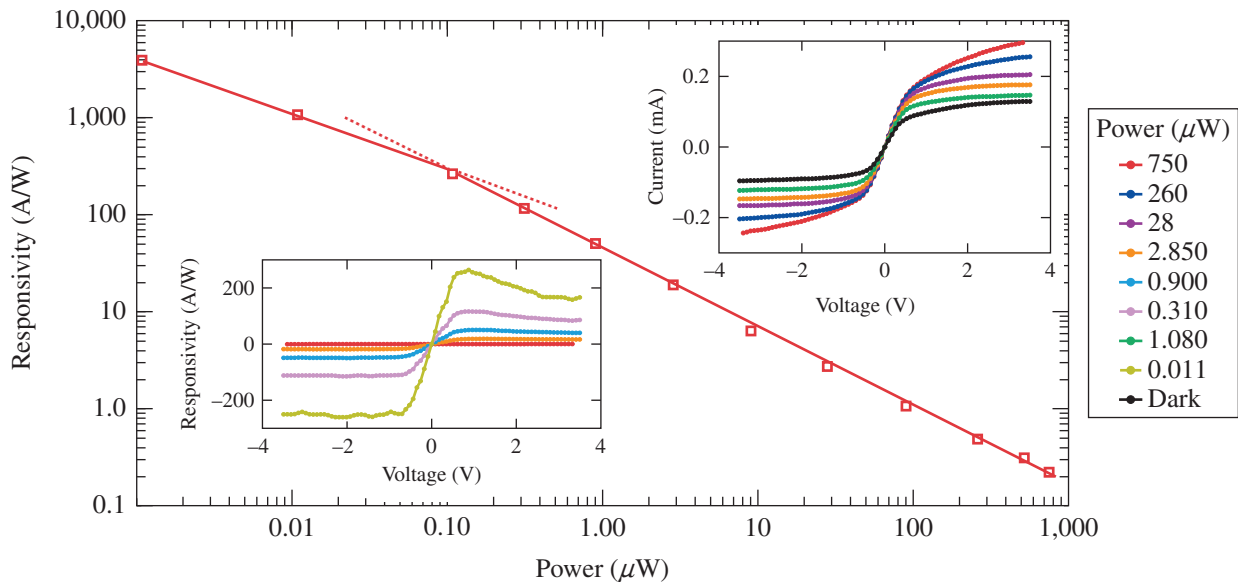
Optical gating in FET's has been recently studied;<sup>5</sup> however, here we have a much simpler structure—an asymmetric nano-channel—and the effect is very strong, even as the incident light power changes in a very narrow range from 1 to 1.4  $\mu\text{W}$ .

The optical gating is caused by photogenerated holes that move to locations below and/or beside the channel and are likely to partly compensate negative surface charges at the walls of the trenches. This effect reduces the channel depletion in an analogous way to a gate voltage in the FET, further opening the 2DEG channel and, consequently, leading to a large optical responsivity. The latter conclusion is in full agreement with the detection efficiency (DE) data presented in the bottom right inset in Fig. 143.43. The DE value increases with the incident light power and the ANCD structure exhibits an intrinsic gain; i.e., a  $\text{DE} \gg 1$ , resulting from the optical gating of the channel of the SSD.

A family of I–V characteristics, this time collected for a normally ON device, is shown in the top right inset in Fig. 143.44 and was measured under light illumination conditions similar to those in Fig. 143.43. We note that now the I–V curve measured in the dark (black dots) has an S-like shape and resembles the one presented in Fig. 143.42(b). The unbiased diode is clearly in the ON state, and when biased, the current is in the mA rather

than the  $\mu\text{A}$  range. The observed nonlinearity (transition toward saturation) comes, as indicated earlier, from the  $\Gamma$ – $L$  electron scattering. Figure 143.44 (main panel) shows that the maximum optical responsivity (red squares), expressed in  $\text{A/W}$  (see also the left bottom panel), increases linearly (red solid line) with decreasing optical power over many orders of magnitude with only very slight tapering at the lowest light power levels, reaching a value of almost 10,000  $\text{A/W}$ , comparable to the gain of avalanche-type, single-photon detectors.

The existence of optical gain in normally ON ANCD's is consistent with a model proposed for photoconductive gain in high-electron-mobility transistors (HEMT's).<sup>6</sup> In this model, the band bending present in the 2DEG of the HEMT captures photoexcited electrons, which transit the channel of the device, while photoexcited holes are pushed away from the 2DEG and become trapped in the substrate or in surface states on the sidewalls of the channel. The value of the photoconductive gain is the ratio of the hole trapping time to the electron transit time. The gain is dependent on the optical power because the density of photogenerated charges affects the potential (as in the case of the normally OFF device) that separates the photo-generated holes from the 2DEG, thereby affecting the hole trapping time. The subpicosecond electron transit time of our ANCD's translates into a very large optical gain.



E24325JR

Figure 143.44 Maximum optical responsivity's (red squares; solid line is a linear fit) dependence on the incident optical power for a normally ON ANCD (channel width  $\sim 300$  nm). The top right inset shows the I–V characteristics collected in the dark (black dots) and under 800-nm cw light illumination for power levels in the range of 750 to 0.11  $\mu\text{W}$ . The bottom left inset presents examples of the responsivity versus the bias voltage.

We have also measured an impulse photoresponse of our normally ON sample using 100-fs-wide pulses from our mode-locked Ti:Al<sub>2</sub>O<sub>3</sub> laser and a 50-GHz-bandwidth oscilloscope readout. The observed strong pulse (not shown) was ~120 ps wide and was followed by damped oscillations. Our measured signals were severely restricted by the limited bandwidth of the sample housing; i.e., inductance of wire bonds and pad capacitance, designed for strictly dc characterization.

### Conclusions

We have shown that ANCD's, originally intended for THz applications, also have very interesting photoresponse properties. In normally OFF devices, where the nanochannel width is defined by the depletion layers and electric-field-controlled, optical illumination plays a role of optical gating, analogous to the gate in FET structures. On the other hand, the physics of the photoresponse gain mechanism in normally ON ANCD's arises from a dramatic difference between a subpicosecond transient time of electrons traveling in the 2DEG nanochannel layer and the microsecond lifetime of holes, optically excited and subsequently pushed toward the substrate. When cooled (to

minimize the dark current), our ANCD's should be practical photon counters. The ANCD's implemented in the InAs or InSb material systems should be especially attractive since they will cover the infrared radiation region, including the most-important telecommunication and thermal-imaging wavelengths.

### ACKNOWLEDGMENT

The work in Rochester was supported in part by a University of Rochester Research Grant and by ARO Grant #W911NF-15-1-0356.

### REFERENCES

1. A. M. Song *et al.*, Appl. Phys. Lett. **83**, 1881 (2003).
2. K. Y. Xu, G. Wang, and A. M. Song, Appl. Phys. Lett. **93**, 233506 (2008).
3. C. Balocco *et al.*, Appl. Phys. Lett. **98**, 223501 (2011).
4. J. Mateos *et al.*, Appl. Phys. Lett. **86**, 212103 (2005).
5. S. Tripathi and S. Jit, J. Appl. Phys. **109**, 053102 (2011).
6. M. A. Romero, M. A. G. Martinez, and P. R. Herczfeld, IEEE Trans. Microw. Theory Tech. **44**, 2279 (1996).